Eliminating Dead Zone in Wireless Power Transfer with Repeater Coil by Power Factor Control

1st Yutaka Shikauchi
Graduate School of Frontier Sciences
The University of Tokyo
Kashiwa, Japan
shikauchi.yutaka22@ae.k.u-tokyo.ac.jp

2nd Ryo Matsumoto
Graduate School of Frontier Sciences
The University of Tokyo
Kashiwa, Japan
matsumoto.ryo19@ae.k.u-tokyo.ac.jp

3rd Sakahisa Nagai
Graduate School of Frontier Sciences
The University of Tokyo
Kashiwa, Japan
nagai-saka@k.u-tokyo.ac.jp

4th Toshiyuki Fujita
Graduate School of Frontier Sciences
The University of Tokyo
Kashiwa, Japan
t-fujita@k.u-tokyo.ac.jp

5th Osamu Shimizu
Graduate School of Frontier Sciences
The University of Tokyo
Kashiwa, Japan
shimizu.osamu@k.u-tokyo.ac.jp

6th Hiroshi Fujimoto
Graduate School of Frontier Sciences
The University of Tokyo
Kashiwa, Japan
fujimoto@k.u-tokyo.ac.jp

2023 IEEE Wireless Power Technology Conference and Expo (WPTCE) | 979-8-3503-3737-2/23/$31.00 ©2023 IEEE | DOI: 10.1109/WPTCE56855.2023.10216172

***Abstract*—Dynamic wireless power transfer (D-WPT) is attracting attention as a way to compensate for the shortcomings of electric vehicles. However, the cost of inverters for D-WPT is high due to the cost of the semiconductor devices and controllers, making it difficult to implement in society. Therefore, a method that can energize multiple repeater coils with a power transmitter coil is known as an effort to reduce costs. However, the repeater coil creates a dead zone in which the power cannot be transferred to the receiver coil. The main cause of the dead zone is the high input impedance of the circuit. This paper proposes a method to eliminate the dead zone by implementing power factor control on the transmitter side. In the proposed method, the frequency of the inverter is controlled to maintain the power factor to one when the receiver coil moves over the transmitter and repeater coil. The frequency of the inverter is determined by the hill climbing algorithm.**

***Index Terms*—Dynamic Wireless Power Transfer, Electric Vehicle, Repeater Coil, Dead Zone, Power Factor Control**

I. Introduction

Wireless power transfer (WPT) is a technology of transmitting electric power to electronic devices such as home appliances and electric vehicles (EVs) without the use of wires [1]–[3]. Two main types of WPT *i.e.* magnetic field, electric field and both have been studied [4]–[6]. These two types are used differently depending on the application. In particular, there are many studies on the magnetic field method for EVs [7]–[9]. In addition to the research to bring out the performance of EVs, research is actively conducted to detect of metallic foreign objects during WPT in each case [10], [11]. Also being conducted to reduce the impact on the human body by the leakage magnetic field [12]. The realization of D-WPT is expected to reduce the weight of batteries installed in EVs and extend their cruising distance [13].

However, the implementation cost of D-WPT is enormous, especially since the semiconductor devices and controllers used in the inverter are expensive [14].

Abdolkhani *et al.* proposed a system to significantly reduce the number of components and cost by using a single switch for both voltage rectification and voltage control [15]. A system was proposed to lower the cost of segment configuration without using many inverters by switching circuits based on a flexible operating strategy [16]. The configuration using a repeater coil has been studied as shown in Fig. 1 (b) [17], [18]. Previous studies suggest that the number of inverters can be reduced by repeater coils and that the constant current characteristics of the LCL network can be used to stabilize the received power [14]. Other studies have identified a phenomenon called the dead zone, in which power transmission becomes difficult in terms of efficiency and power when the transmission and repeater coils are arranged horizontally [19]. This dead zone needs to be improved because it has a negative impact on the ability to reduce the number of inverters.

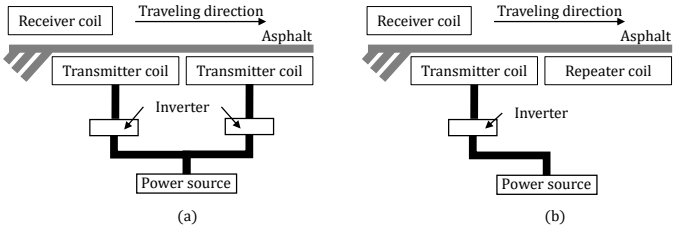

Fig. 1. D-WPT system. (a) System with transmitter and receiver coils. (b) System with transmitter, receiver and repeater coils.

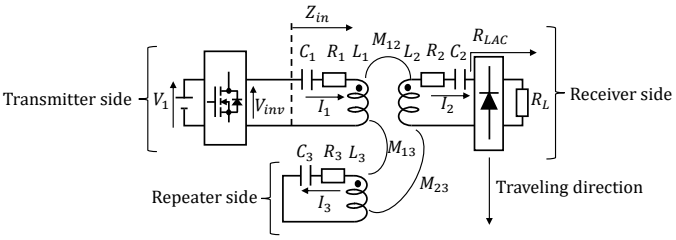

Fig. 2. Configuration of D-WPT circuit with repeater coil.

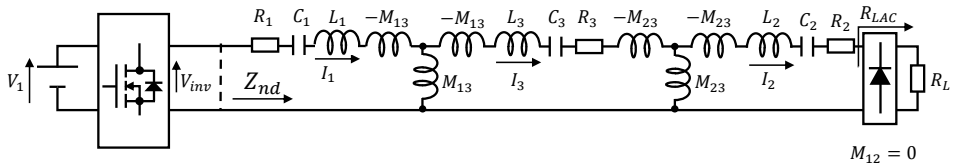

Fig. 3. Equivalent circuit of the D-WPT system with a repeater coil ($M_{12} = 0$).

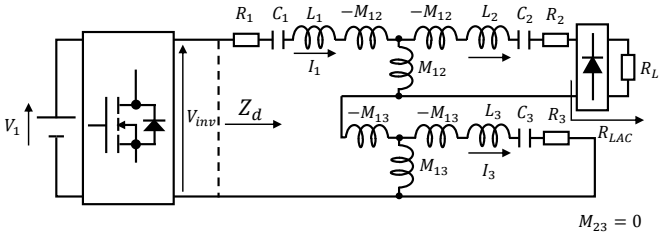

Fig. 4. Equivalent circuit of the D-WPT system with a repeater coil ($M_{23} = 0$).

This paper proposes transmitter side power factor control to eliminate the dead zone. This method determines the frequency depending on the location of the receiver coil and decreases high input impedance which is the cause of the dead zone. Experimental results show that the proposed method improves the received power and efficiency at the dead zone compared to the case where the frequency is constant.

II. Overview of Repeater Coil System

Fig. 2 shows the equivalent circuit of a D-WPT circuit using a repeater coil. Fig. 3 shows the equivalent circuit when the receiver coil is located above the repeater coil. Fig. 4 shows the equivalent circuit when the receiver coil is located above the transmitter coil. Table I shows the definitions of the parameters used in this paper. The subscripts i and j in Table I are 1, 2, and 3, where 1 indicates the transmitter side, 2 indicates the receiver side, and 3 indicates the repeater side, respectively. Also, (i, j) is expressed as a combination of (1, 2), (1, 3), and (2, 3), indicating the transmitter-receiver, transmitter-repeater, and receiver-repeater sides respectively. Table Ⅱ shows the parameters used in the theoretical calculations.

X_i, M_{ij} and R_{LAC} can be expressed as

$$X_i = \omega L_i - \frac{1}{\omega C_i} \quad i \in \{1, 2, 3\}, \tag{1}$$

$$M_{ij} = k_{ij}\sqrt{L_i L_j} \quad i \in \{1, 2, 3\} \quad j \in \{1, 2, 3\}, \tag{2}$$

$$R_{LAC} = \frac{8}{\pi^2} R_L. \tag{3}$$

The circuit equation is formulated based on Fig. 2 as

$$\begin{bmatrix} V_{inv} \\ 0 \\ 0 \end{bmatrix} = \begin{bmatrix} R_1 + jX_1 & j\omega M_{12} & j\omega M_{13} \\ j\omega M_{12} & R_2 + R_{LAC} + jX_2 & j\omega M_{23} \\ j\omega M_{13} & j\omega M_{23} & R_3 + jX_3 \end{bmatrix} \begin{bmatrix} I_1 \\ I_2 \\ I_3 \end{bmatrix}. \tag{4}$$

From (4), P_{out} can be defined as

$$P_{out} = R_{LAC} I_2^2. \tag{5}$$

TABLE I
Nomenclature.

Parameter	Symbol
Source voltage	V_1
Output voltage of inverter	V_{inv}
Coil current	I_i
Coupling coefficient	k_{ij}
Mutual inductance	M_{ij}
Self inductance of coil	L_i
Resonance capacitor	C_i
Reactance of L_i and C_i	X_i
Coil winding resistance	R_i
Load resistance	R_L
AC equivalent load resistance	R_{LAC}
Operating Angular frequency	ω
Operating Angular frequency of the proposed method	ω_{prop}
Operating frequency	f
Operating frequency of the proposed method	f_{prop}
The resonance frequency of each side	f_i
Variation step of operating frequency	Δf
Input impedance of the entire circuit	Z_{in}
Input impedance of circuit then dead zone ($M_{23} = 0$)	Z_d
Input impedance of circuit then dead zone ($M_{12} = 0$)	Z_{nd}
Angular declination of V_{inv} and I_1	θ
AC-AC efficiency	η
Power consumed at R_{LAC}	P_{out}

TABLE II
Theory And Simulation Parameters.

Parameter	Symbol	Value
Source voltage	V_1	100 V
Operating frequency	f	85.0 kHz
Resonance frequency of transmitter side	f_1	85.0 kHz
Resonance frequency of receiver side	f_2	85.0 kHz
Resonance frequency of repeater side	f_3	85.0 kHz
Self inductance of transmitter side coil	L_1	137 µH
Self inductance of receiver side coil	L_2	55 µH
Self inductance of repeater side coil	L_3	137 µH
Transmitter side capacitor	C_1	25.591 nF
Receiver side capacitor	C_2	63.744 nF
Repeater side capacitor	C_3	25.591 nF
Transmitter side resistance	R_1	75 mΩ
Receiver side resistance	R_2	35 mΩ
Repeater side resistance	R_3	75 mΩ
Load resistance	R_L	22.3 Ω

III. Power transfer issue with repeater coil

A. Negative Impact on Power Consumed at Dead Zone

The dead zone indicates the location of the receiver coil where little power is received. The effect of this is shown in Fig. 5. The value of maximum P_{out} in the dead zone is about 35.1 W when the receiver coil is above the transmitter coil.

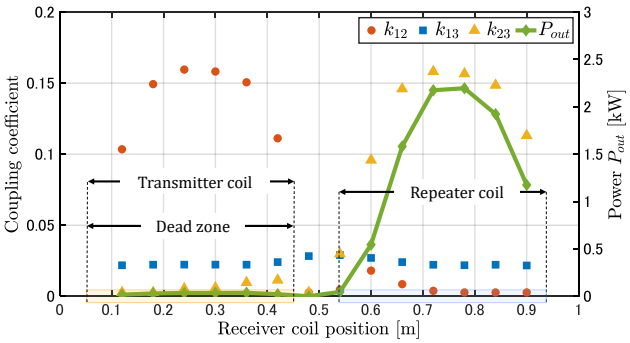

Fig. 5. Coupling coefficient and P_{out} for receiver coil positions.

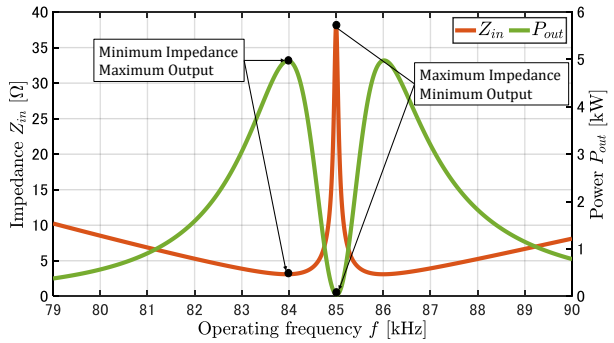

Fig. 6. Z_{in} and P_{out} when f is varied from 79 kHz to 90 kHz in the dead zone ($M_{12} = 0.158$, $M_{13} = 0.022$, $M_{23} = 0.0021$).

On the other hand, when the receiver coil is above the repeater coil, P_{out} increases to 2.2 kW in theory.

B. Cause of Dead Zone

The dead zone is caused by a larger Z_{in}. In the following analysis, it is assumed that the circuit is driven at its resonant frequency as in the conventional method [20] as

$$\omega = \frac{1}{\sqrt{L_1C_1}} = \frac{1}{\sqrt{L_2C_2}} = \frac{1}{\sqrt{L_3C_3}} = 2\pi f. \tag{6}$$

From (6), when the receiver coil is located in the dead zone, Z_d in Fig. 4 can be expressed as shown as

$$Z_d = R_1 + jX_1 + \frac{(\omega M_{12})^2}{(R_2 + R_{LAC}) + jX_2} + \frac{(\omega M_{13})^2}{R_3 + jX_3}. \tag{7}$$

Assuming that the internal resistance is very small and substituting $R_1 = R_2 = R_3 = 0$ into (7), Z_d diverges to infinity. On the other hand, Z_d does not diverge to infinity when applying the parameters in Table Ⅱ because R_1, R_2, and R_3 are not zero. Fig. 6 shows P_{out} and Z_{in} when f is varied from 79 kHz to 90 kHz at the dead zone ($M_{12} = 0.158$, $M_{13} = 0.022$, $M_{23} = 0.0021$). When f is 85 kHz, Z_{in} reaches its maximum value and P_{out} reaches its minimum value. In other words, it is considered that the minimum value of P_{out} in the dead zone is reached when Z_{in} reaches its maximum value. As shown in Fig. 7, there are three points of frequencies in which the power factor on the transmitter side is one. Among them, P_{out} reaches its minimum value at 85 kHz, and P_{out} reaches its maximum value at 84 kHz and 86 kHz. Similarly, when the receiver coil is located in the non-dead zone, Z_{nd} in Fig. 3 can be expressed as

$$Z_{nd} = R_1 + jX_1 + \frac{(\omega M_{13})^2}{R_3 + jX_3 + \frac{(\omega M_{23})^2}{(R_2 + R_{LAC} + jX_2)}}. \tag{8}$$

Substituting R_1=R_2=R_3=0 into (8), Z_{nd} does not diverge to infinity.

IV. Proposed Method

The cause of the dead zone is that Z_{in} becomes high when the switching frequency of the inverter matches the circuit's resonant frequency. Therefore, the proposed method

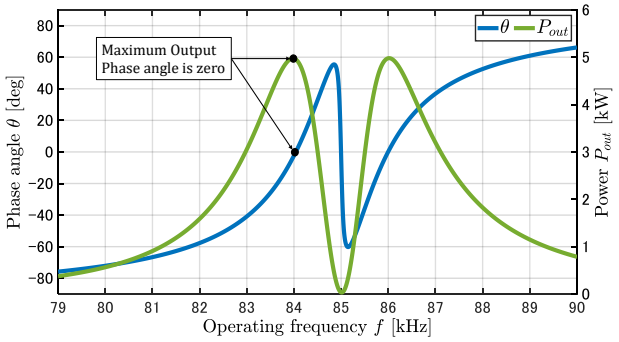

Fig. 7. θ and P_{out} when f is varied from 79 kHz to 90 kHz in the dead zone ($M_{12} = 0.158$, $M_{13} = 0.022$, $M_{23} = 0.0021$).

is to minimize Z_{in} and adjust the power factor to one by controlling the switching frequency of the inverter. In order to do so, it is necessary to find the frequency of the power supply such that the imaginary part of the impedance is zero. The calculations are performed under $R_1 = R_2 = R$ and $X_1 = X_3 = X$. From Fig. 2, the transmitter side current I_1

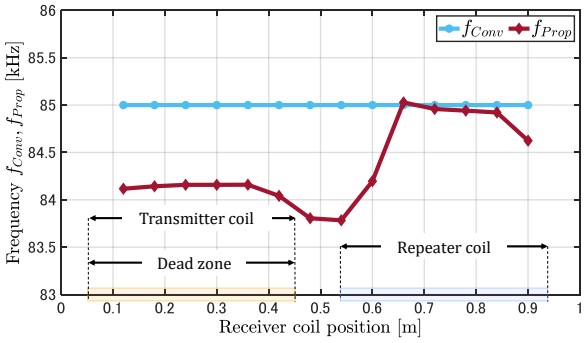

Fig. 8. Comparison of frequencies in proposed method and conventional method for receiver coil positions.

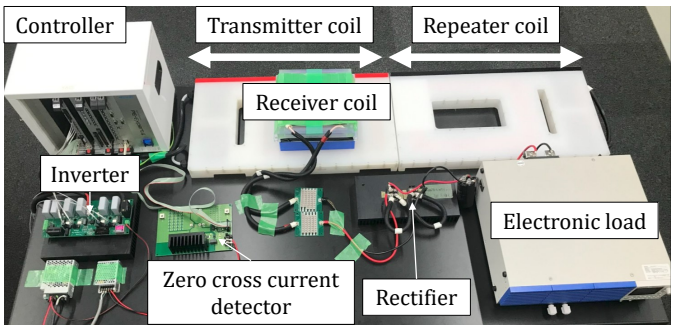

Fig. 9. Experimental setting.

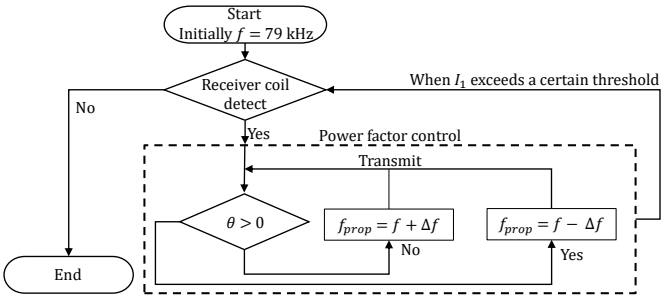

Fig. 10. Flowchart for power factor control on transmitter side.

can be derived as

$$I_1(\omega) = \frac{dV_{inv}}{a+b-c}, \tag{9}$$

$$a = \{(R+jX)^2 + (\omega M_{13})^2\}(R_2 + R_{LAC} + jX_2), \tag{10}$$

$$b = (\omega^2 M_{12}^2 + \omega^2 M_{23}^2)(R+jX), \tag{11}$$

$$c = 2j\omega M_{12} M_{13} M_{23}, \tag{12}$$

$$d = (R+jX)(R_2 + R_{LAC} + jX_2) + (\omega M_{23})^2. \tag{13}$$

ω_{prop} denotes the frequency at which the transmitter side power factor is set to one. The purpose of this paper is to eliminate the dead zone by minimizing Z_{in} and achieve the maximum value of P_{out} by using ω_{prop}. The equations for setting the imaginary parts of Z_{in} to zero are shown as

$$\mathrm{Im}\left[\frac{V_{inv}}{I_1(\omega_{prop})}\right] = 0. \tag{14}$$

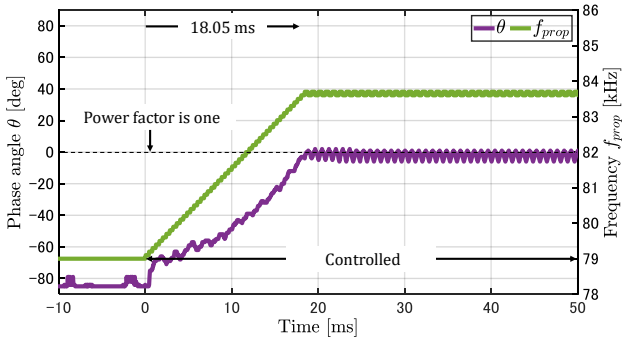

Fig. 11. Experimental results of transmitter power factor control of power supply frequency when applying the proposed method in a dead zone and the receiver coil position is 0.2 m.

TABLE III
EXPERIMANTAL PARAMETERS.

Parameter	Symbol	Value
Source voltage	V_1	20 V
Resonance frequency of transmitter side	f_1	85.1 kHz
Resonance frequency of receiver side	f_2	85.2 kHz
Resonance frequency of repeater side	f_3	85.1 kHz
Variation step of operating frequency	Δf	100 Hz
Self inductance of transmitter side coil	L_1	138.3 µH
Self inductance of receiver side coil	L_2	54.7 µH
Self inductance of repeater side coil	L_3	139.4 µH
Transmitter side capacitor	C_1	25.3 nF
Receiver side capacitor	C_2	63.8 nF
Repeater side capacitor	C_3	25.1 nF
Transmitter side resistance	R_1	77.2 mΩ
Receiver side resistance	R_2	34.7 mΩ
Repeater side resistance	R_3	72.5 mΩ
Load resistance	R_L	22.3 Ω

V. EXPERIMENT

A. Experimental Procedure

In the experiment, the proposed method is compared to the conventional method in which the frequency of the inverter is fixed to the resonant frequency. Fig. 8 shows the comparison of frequencies in the proposed method and the conventional method from equation (14). ω_{prop} can be obtained for the transmitter side power factor to be one [21], but the values of k_{ij} and R_L are required. Therefore, an experiment is conducted using the hill climbing algorithm to detect the phase of V_{inv} and I_1 to determine ω_{prop} so that they are in phase without using the values of k_{ij} and R_L. Fig. 9 shows the experiment setting. In the experiment, η and P_{out} are compared between the proposed method and the conventional method. The parameters in Table III are used in the experiment.

B. Experimental and Simulation Results

1) Frequency control results: Fig. 10 shows the flowchart for the power factor control on the transmitter side. θ is detected and the frequency is controlled so that θ becomes zero. When θ is in phase lead, the frequency is increased by Δf, and when θ is in phase delay, the frequency is decreased by Δf. Fig. 11 shows the trajectories of θ and f_{prop} when the receiver coil position is 0.2 m. The iteration period of the hill climbing algorithm is set to 0.4 ms. The frequency of the inverter is initially set to 79 kHz. As shown in Fig. 7, the ideal power factor and the maximum output power can be obtained when the switching frequency is 84 kHz. Therefore, the initial frequency is set to a value lower than 84 kHz to ensure the convergence of the frequency control. The results in Fig. 11 show that it took 18.05 ms for θ to reach zero. Also,

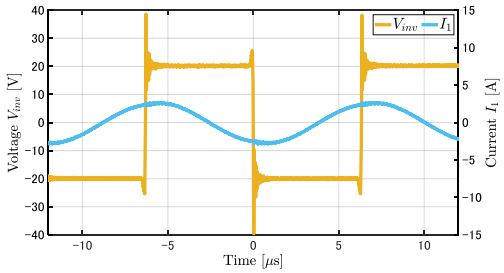

(a) Initial phase condition (f=79 kHz).

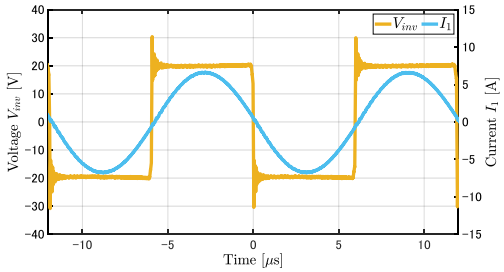

(b) Proposed method (With power factor control).

Fig. 12. Experimental results of waveforms of V_{inv} and I_1 in the proposed and conventional methods.

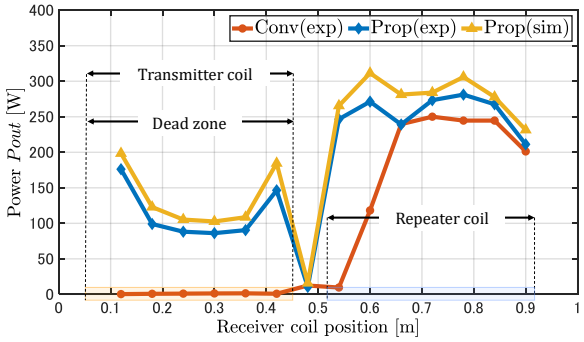

Fig. 13. Experimental results of comparison of P_{out} between proposed and conventional method.

the peak-to-peak value of θ after convergence was 10 deg. Fig. 12 shows V_{inv} and I_1 without the power factor control. θ is not zero due to the effect of resonance mismatch, but in the proposed method, it was confirmed that θ is controlled to be close to zero.

2) Measured Efficiency and Received Power: The results of P_{out} and η when applying the proposed and conventional methods are shown in Figs. 13 and 14, respectively. The experiment was conducted at low power. Fig. 14 shows that the average power in the dead zone is 11.2 W for the conventional method. However, it was confirmed that the proposed method improves the average power to 108.9 W. In addition, as shown in Fig. 14, the average η of the dead zone improved from 11.5% to 93.4% by applying the proposed method. The simulation results show almost the same trend, although it is

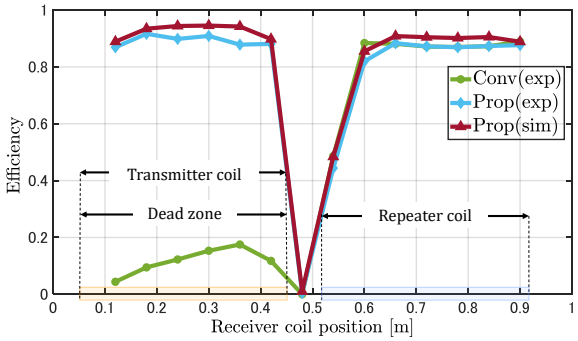

Fig. 14. Experimental results of comparison of η between proposed and conventional method.

slightly different from the experimental results. There are two possible reasons for the discrepancy. Firstly, the parameters in Table Ⅲ may be different from the actual values due to measurement errors. Secondly, θ does not converge exactly to zero degrees due to the step size of the hill climbing method. However, These results suggest that the proposed transmitter side power factor control is effective in eliminating the dead zone.

VI. Conclusions

This paper proposes a method of eliminating the dead zone that occurs in D-WPT with a repeater coil. The dead zone is a section where received power is substantially reduced, and it is shown that the cause of the dead zone is a high input impedance. Therefore, a method was proposed to minimize the input impedance above the dead zone by controlling the operating frequency and maintaining the power factor to one on the transmitter side. In the experiment, the received power and the transmission efficiency were measured in comparison with the conventional method in which the switching frequency is fixed to the circuit's resonant frequency. As a result, it was confirmed that the proposed method improved the average of power consumed at the dead zone from 11.2 W to 108.9 W, and increased the transmission efficiency from 11.5% to 93.4%.

Acknowledgment

This work was partly supported by JST-Mirai Program Grant Number JPMJMI21E2 and the New Energy and Industrial Technology Development Organization (NEDO) Project Number JPNP21005, Japan.

References

[1] A. Bilal, S. Kim, F. Lin and G. Covic, "Analysis of IPT Intermediate Coupler System for Vehicle Charging Over Large Air Gaps," in IEEE Journal of Emerging and Selected Topics in Industrial Electronics, vol. 3, no. 4, pp. 1149-1158, Oct. 2022.

[2] L. Wu, B. Zhang, Y. Jiang and J. Zhou, "A Robust Parity-Time-Symmetric WPT System With Extended Constant-Power Range for Cordless Kitchen Appliances," in IEEE Transactions on Industry Applications, vol. 58, no. 1, pp. 1179-1189 Jan.-Feb. 2022.

[3] B. Zhang, J. Deng, L. Li, Z. Wang, S. Wang and G. Guidi, "Thermal Analysis and Design of a 30kW EV Wireless Charger with Liquid-Cooled Shell for Magnetic Coupler and Integrated Power Converter," 2021 IEEE Applied Power Electronics Conference and Exposition (APEC), Phoenix, AZ, USA, pp. 426-431, 2021.

[4] Y. Yamada, S. Hasegawa, T. Imura and Y. Hori, "Design Method of Coreless Coil Considering Power, Efficiency and Magnetic Field Leakage in Wireless Power Transfer," IECON 2022 – 48th Annual Conference of the IEEE Industrial Electronics Society, Brussels, Belgium, pp. 1-6, 2022.

[5] T. Chen, C. Cheng, H. Cheng, C. Wang and C. C. Mi, "Load-Independent Power-Repeater Capacitive Power Transfer System With Multiple Constant Voltage Outputs," in IEEE Journal of Emerging and Selected Topics in Power Electronics, vol. 10, no. 5, pp. 6358-6370, Oct. 2022.

[6] J. -Q. Zhu, Y. -L. Ban, R. -M. Xu and C. C. Mi, "An NFC-Connected Coupler Using IPT-CPT-Combined Wireless Charging for Metal-Cover Smartphone Applications," in IEEE Transactions on Power Electronics, vol. 36, no. 6, pp. 6323-6338, June. 2021.

[7] B. J. Varghese, A. Kamineni, N. Roberts, M. Halling, D. J. Thrimawithana and R. A. Zane, "Design Considerations for 50 kW Dynamic Wireless Charging with Concrete-Embedded Coils," 2020 IEEE PELS Workshop on Emerging Technologies: Wireless Power Transfer (WoW), Seoul, Korea (South), pp. 40-44, 2020.

[8] T. Fujita, S. Nagai, O. Shimizu, H. Fujimoto and Y. Ohmori, "Resonant Capacitor Voltage Based 85-kHz 3-kW Synchronous Rectification on Wireless Power Transfer System," 2022 Wireless Power Week (WPW), Bordeaux, France, 2022.

[9] K. Kusaka, J. Itoh, "Development Trends of Inductive Power Transfer System Utilizing Electromagnetic Induction with Focus on Transmission Frequency and Transmission Power," IEEJ J. Ind. Appl., vol.6, No.5, pp.328-339, 2017.

[10] J. W. Jeong, S. H. Ryu, B. K. Lee, and H. J. Kim, "Tech tree study on foreign object detection technology in wireless charging system for electric vehicles," INTELEC, International Telecommunications Energy Conference (Proceedings), vol. 2016-Septe, pp. 1–4, 2016.

[11] Y. Deguchi, S. Nagai, T. Fujita, H. Fujimoto and Y. Hori, "Sensorless Metal Object Detection Using Transmission-Side Voltage Pulses in Standby Phase for Dynamic Wireless Power Transfer," 2021 IEEE PELS Workshop on Emerging Technologies: Wireless Power Transfer (WoW), San Diego, CA, USA, pp. 1-5, 2021.

[12] H. Sumiya, E. Takahashi, N. Yamaguchi, K. Tani, S. Nagai, T. Fujita, and H. Fujimoto, "Coil scaling law of wireless power transfer systems for electromagnetic field leakage evaluation for electric vehicles," IEEJ J. Ind. Appl., vol. 10, no. 5, pp. 575–576, 2021.

[13] H. Fujimoto, O. Shimizu, S. Nagai, T. Fujita, D. Gunji and Y. Ohmori, "Development of Wireless In-whinl Motors for Dynamic Charging: From 2nd to 3rd generation," 2020 IEEE PELS Workshop on Emerging Technologies: Wireless Power Transfer (WoW), Seoul, Korea (South), pp. 56-61, 2020.

[14] W. Xiong, Q. Yu, Z. Liu, L. Zhao, Q. Zhu and M. Su, "A Detuning-Repeater-Based Dynamic Wireless Charging System With Quasi-Constant Output Power and Reduced Inverter Count," in IEEE Transactions on Power Electronics, vol. 38, no. 1, pp. 1336-1347, 2023.

[15] A. Abdolkhani, "Single-switch soft-switched power flow controller for wireless power transfer applications," 2017 IEEE Wireless Power Transfer Conference (WPTC), Taipei, Taiwan, pp. 1-4, 2017.

[16] C. Cai, M. Saeedifard, J. Wang, P. Zhang, J. Zhao and Y. Hong, "A Cost-Effective Segmented Dynamic Wireless Charging System With Stable Efficiency and Output Power," in IEEE Transactions on Power Electronics, vol. 37, no. 7, pp. 8682-8700, July. 2022.

[17] W. X. Zhong, C. K. Lee, and S. Y. R. Hui, "General analysis on the use of tesla's resonators in domino forms for wireless power transfer," IEEE Transactions on Industrial Electronics, 2011.

[18] J. W. Kim et al., "Wireless power transfer for free positioning using compact planar multiple self-resonators," 2012 IEEE MTT-S International Microwave Workshop Series on Innovative Wireless Power Transmission: Technologies, Systems, and Applications, Kyoto, Japan, pp. 127-130, 2012.

[19] K. E. Koh, T. Imura, and Y. Hori, "Analysis of Dead Zone in Wireless Power Transfer via Magnetic Resonant Coupling for Charging Moving Electric Vehicles," Int. Journal of Intelligent Transportation Systems Research, Feb. 2015.

[20] C. Wang, P. Wang, Q. Zhu and M. Su, "An Alternate Arrangement of Active and Repeater Coils for Quasi-Constant Power Wireless EV Charging," 2019 IEEE PELS Workshop on Emerging Technologies: Wireless Power Transfer (WoW), London, UK, pp. 313-317, 2019.

[21] R. Matsumoto and H. Fujimoto, "Adaptive Compensation Scheme for Wireless Power Transfer Systems with Coil Inductance Variation Using PWM-Controlled Switched Capacitor," 2022 Wireless Power Week (WPW), Bordeaux, France, 2022.